Available online at www.sciencedirect.com

SciVerse ScienceDirect

Ceramics International 38 (2012) 3419–3425

CERAMICS INTERNATIONAL

www.elsevier.com/locate/ceramint

Microstructure and ablation behaviors of integer felt reinforced C/C–SiC–ZrC composites prepared by a two-step method

Zhaoqian Li, Hejun Li *, Shouyang Zhang, Kezhi Li

State Key Laboratory of Solidification Processing, Carbon/Carbon Composites Research Center, Northwestern Polytechnical University, Xi'an 710072, PR China

Received 27 October 2011; received in revised form 30 November 2011; accepted 19 December 2011
Available online 28 December 2011

Abstract

To satisfy the increasing demand for advanced materials with temperature capability of over 2000 °C for ultrahigh temperature and aerospace applications, integer felt reinforced C/C–SiC–ZrC composites were prepared by isothermal chemical vapor infiltration (ICVI) combined with reaction melt infiltration (RMI) method. The microstructure and ablation properties of the felt-based C/C–SiC–ZrC composites were investigated. The ablation test was carried out under an oxyacetylene torch flame. The results indicate that the linear and mass ablation rates of the integer felt reinforced C/C–SiC–ZrC prepared are greatly reduced compared with those of C/C composites and the co-addition of ZrC and SiC into C/C composites effectively enhances their ablation resistance.

Keywords: C. Corrosion; E. Thermal applications; C/C–SiC–ZrC composites; Reaction melt infiltration

1. Introduction

Carbon/carbon (C/C) composites possessing excellent properties such as low density, high specific strength, high thermal conductivity, resistance to thermal shock and ablation are considered as one of the most promising materials for high temperature applications [1–4]. However, there is an increasing demand for advanced materials with temperature capability of over 2000 °C for ultrahigh temperature and aerospace applications, such as rocket engines, nose cones and leading edges of hypersonic and re-entry type vehicles [5,6]. The rapid oxidation and ablation of C/C composites at the eroding of the ultrahigh temperature and high pressure flux have seriously limited their application in advanced space systems [7,8]. It is necessary to improve the ablation resistance of C/C composites in an oxidizing atmosphere at high temperature.

A survey of literature [9–12] suggests that significant research has been carried out on introducing refractory carbide/boride ceramics (e.g. ZrC, HfC, TaC, ZrB_2, etc.) into C/C matrix to obtain composites with improved ablation resistance. ZrC is an advanced ceramic with a high melting point (3540 °C), excellent chemical stability and resistance to thermal shock [13,14]. In addition, its oxide can effectively reduce the diffusion of oxygen. Shen et al. [9] prepared ZrC doped C/C composites using liquid precursor impregnation and thermal gradient chemical vapor infiltration (TCVI) process. Tong et al. [11] prepared pitch-derived ZrC/C composites using Zr-containing pitch by hot-pressed technology and the effect of the content of Zr and the dimension of particles on the ablation behavior of composites up to 3000 °C was studied. Wang et al. [15] prepared C/C–ZrC composites by RMI process and studied their reaction kinetics and ablation properties. Introducing ZrC into C/C composites has initially shown its advantage in the improvement of ablation resistance.

In order to further improve the ablation resistance of C/C–ZrC composites, SiC was added into the matrix by putting Si in the infiltration powders. During infiltration process, Si addition could improve the wettability between molten Zr and C/C composites as well as react with C to form SiC in the matrix. Under oxidizing environment, SiC can be oxidized to SiO_2 oxide that has a melting point of 1723 °C. At an ablation temperature higher than 2000 °C, molten SiO_2 is expected to bond with ZrO_2 to seal the cracks and protect the fibers inside. In this paper, integer felt reinforced C/C–SiC–ZrC composites were prepared by ICVI combined with RMI method. The microstructure and ablation properties of the C/C–SiC–ZrC composites were investigated in detail.

* Corresponding author. Tel.: +86 29 88495004; fax: +86 29 88492642.
E-mail address: lihejun@nwpu.edu.cn (H. Li).

0272-8842/$36.00
doi:10.1016/j.ceramint.2011.12.054

2. Experimental procedure

2.1. Material preparation

The porous integer felt reinforced C/C skeleton with a density of 1.35 g/cm^3 were prepared by the process of isothermal chemical vapor infiltration (ICVI) to densify the carbon fiber needled integer felt with a density of 0.17 g/cm^3. Fig. 1 shows the schematic diagram of the ICVI process. During ICVI process, CH_4 was used as the precursor with a flow rate of 5–10 L/min and the furnace operated at 1050–1150 °C under the pressure of 5–15 kPa for 30–40 h. Then the composites were graphitized at 2500 °C for 2 h in an inert atmosphere. All samples, with a size of Ø30 mm × 10 mm, were polished with 400 and 800 grit SiC paper firstly and then cleaned ultrasonically with ethanol and dried at 100 °C for 2 h.

The integer felt reinforced C/C–SiC–ZrC composites was prepared by a new RMI process with Zr, Si, C and ZrO_2 powders in argon at 2300 °C for 2 h. The precursor powders were mixed as $3Zr{\cdot}5Si{\cdot}C{\cdot}0.2ZrO_2$ mole ratio. Then as-produced C/C composites were embedded in the pack mixture in a graphite crucible and then put into an electric furnace. The furnace was heated up to 2300 °C, with a heating rate of 9 °C/min, kept at that temperature for 2 h, and then cooled down to room temperature with a cooling rate of 4 °C/min. The whole heat-treatment was carried out in an argon protective atmosphere.

2.2. Mechanical tests

To study the mechanical properties of the composites, 3-points bending test was performed on an electronic universal testing machine (CMT 5304, Suns Co. China). The load velocity was 0.05 mm/min. The effective size of the samples was 40 mm × 10 mm × 4 mm. The number of specimens used in the tensile test was not less than five.

2.3. Ablation tests

The ablation behavior of integer felt reinforced C/C–SiC–ZrC composites was tested with an oxyacetylene flame, which is close to the practical ablative situation for aerospace materials. During the test, the samples with a size of Ø30 mm × 10 mm were exposed to the flame. The pressure and flux of O_2 were 0.4 MPa and 0.21 L/s, and those of C_2H_2 were 0.095 MPa and 0.155 L/s, respectively. The inner diameter of the nozzle was 2 mm and the distance between the nozzle tip and the sample was 10 mm. Sample was fixed in a water cooled copper concave fixture and exposed to the flame in the atmosphere for 20 s, 30 s and 60 s, respectively. The highest temperature of the oxyacetylene flame that was measured by an optical pyrometer reached as high as 2300 °C. The ablation performance was evaluated through the linear ablation rate and mass ablation rate. The final ablation rates of the samples were the average of no less than three samples.

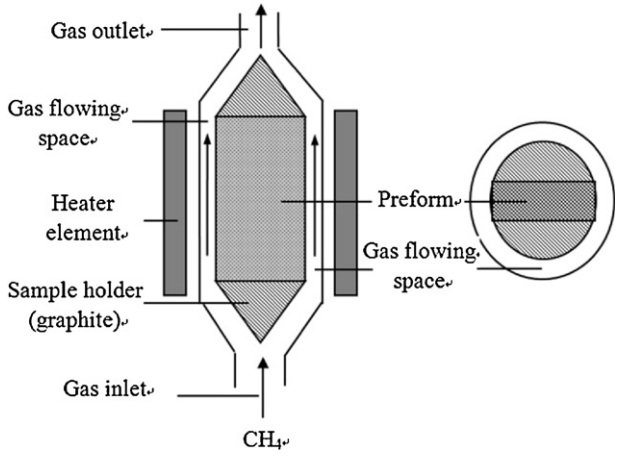

Fig. 1. Schematic diagram of the ICVI process.

2.4. Characterization

Phase analysis of integer felt reinforced C/C–SiC–ZrC composites was carried out by X-ray diffraction (XRD, Philips X' Pert MPD, Holland) using Cu as anode material and graphite monochromator. The microstructure and morphology of the composites were analyzed by a field emission scanning electron microscopy (FESEM, Zeiss-Supra 55) combined with an energy dispersive spectroscopy (EDS, Oxford-INCAPenta-FET_3) for chemical analysis. The density of the samples was measured with the Archimedes method.

3. Results and discussion

3.1. Microstructure of the composites

Comparing with two-dimensional (2D) and three-dimensional (3D) carbon fiber perform, integer felt perform has a more uniform fiber distribution. Therefore, in order to prepare the porous C/C skeleton with a uniform porosity distribution, carbon fiber needled integer felt perform was used as reinforcement of the C/C–SiC–ZrC composites in this study. The integer felt perform was firstly infiltrated with carbon by ICVI process to form a porous C/C skeleton. The density of the as-prepared porous C/C skeleton was controlled to be 1.35 g/cm^3. Fig. 2 shows the morphology of the porous integer felt reinforced C/C composites. Fig. 1(a) displays that the as-prepared composites have homogeneous microstructure and uniform porosity distribution. During ICVI process, pyrolytic carbon (PyC) uniformly deposited on the surface of the fibers of the integer felt and the large holes among the fibers were not fully filled with PyC, so voids were formed. The morphology of individual fibers is shown in Fig. 1(b). It is clear that the thickness of PyC on the surface of fibers is about 10 μm and the fibers distribute disorderly. The continuous open voids that mainly distribute among carbon fibers can be conjectured to be the accesses for the infiltration of molten powders during RMI process.

Fig. 3 shows the XRD patterns of C/C–SiC–ZrC composites. Fig. 3(a) reveals that the surface of the composites is composed of SiC and ZrC. It is noticeable that no C peck is seen on the XRD pattern, which means that the surface of the composites is completely covered by SiC and ZrC layer. During RMI process,

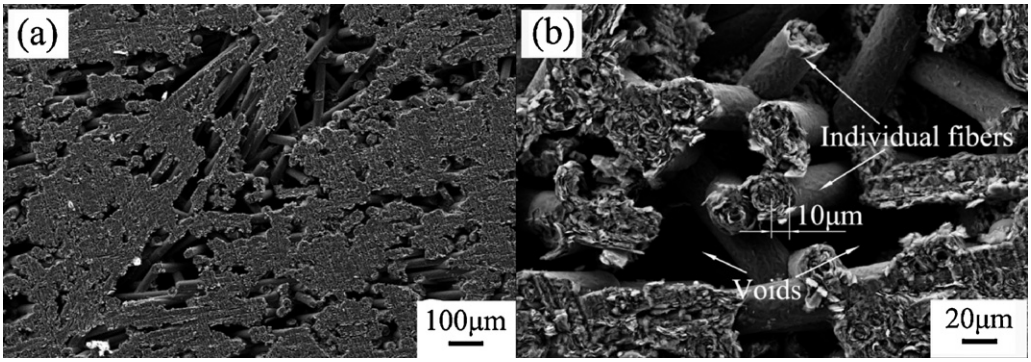

Fig. 2. Morphology of the porous integer felt reinforced C/C composites: (a) voids distribution; (b) magnification of (a).

Si and Zr powders have reacted with C contained in precursor powders and C/C matrix. The following reactions would happen [16,17]:

$$Si(l) + C(s) = SiC(s) \quad (1)$$

$$Zr(l) + C(s) = ZrC(s) \quad (2)$$

Fig. 4(a)–(d) shows the microstructure and EDS analysis of the C/C–SiC–ZrC composites in different positions. It is clear that the structure of the composites is gradiently changed from dense outer layer to the porous internal layer. The surface of the composites (Fig. 2(a)) is covered by a dense coating that is composed of two kinds of crystalline particles characterized as grey and white in the coating. By EDS analysis, the grey and white phases can be distinguished as SiC and ZrC, respectively, which was in accordance with the XRD result. Cross-section SEM image (Fig. 4(b)) shows that the ZrC–SiC coating on the surface was about 80 μm in thickness without penetrable cracks or large holes because all the cracks can be prevented by the crystal particles of ZrC. The composition variations of C, Si and Zr are shown in Fig. 5. It is clear that the phases of SiC and ZrC disperse equably in the coating and many have infiltrated into the interior of the composites and that the content of element Si in the transition layer and on the surface of the coating is higher than that in other areas. The distribution of element Si, representing SiC, at the bonding site and in the interior of the matrix leads to the good combination between the coating and

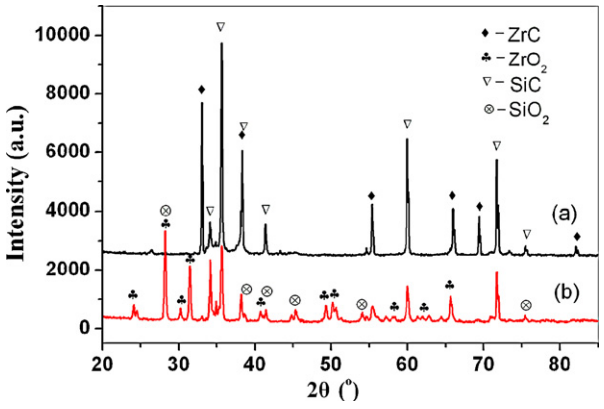

Fig. 3. XRD patterns of the integer felt reinforced C/C–SiC–ZrC composites before (a) and after (b) ablation.

matrix, because the CTE of SiC is similar to that of C/C composites. The ZrC–SiC coating acts as an oxygen diffusion barrier for C/C–SiC–ZrC composites and reacts with oxygen to form zirconium dioxide (ZrO_2) and silicon dioxide (SiO_2) in oxyacetylene flame, which grows rapidly in volume to plug the cracks, preventing the substrate's ablation in this way. Therefore, the dense ZrC–SiC coating that can be obtained by RMI process is expected to have a better anti-ablation property for C/C–SiC–ZrC composites.

Individual carbon fibers after infiltration can be seen in Fig. 4(c) and (d), which are located at the inner and center position of the composites, respectively. The interesting feature is that the surface of the individual carbon fibers is also covered by a dense coating composed of ZrC and SiC, and these particles are not simply physically adhered to the fiber surfaces but truly chemically bonded to the fiber surfaces due to the participation of carbon from the fiber surface in the active carbothermal reaction. During the heat treatment of RMI process, Si and Zr in the original precursor powders melted and penetrated readily into the porous C/C skeleton obtained by ICVI process. Simultaneously, SiC and ZrC were formed by the in situ carbothermal reaction between Si, Zr and C contained in the matrix. Fig. 4(b)–(d) also indicate that the amount of SiC and ZrC formed inside the composites reduces gradually with the increase of infiltration depth, which leads to the increase of the residual voids. The matrix under the coating is very dense, still many white ZrC phases exist on the surface of inner fibers but only a small amount of ZrC particles form on the surface of center fibers. This could be attributed to the in situ reaction occurring to molten Si and Zr during their infiltration into the porous C/C matrix, the formation of SiC and ZrC closing the open pore structure at the front surface and preventing further infiltration.

3.2. Mechanical properties of the composites

The apparent density and bending properties of C/C and C/C–SiC–ZrC composites are shown in Table 1. It displays that the apparent density and bending strength of the C/C–SiC–ZrC composites increase by about 51.1% and 9.33% than those of C/C composites, respectively.

The reinforcing mechanisms of the composites were studied via stress–strain curves and SEM morphology analysis (Fig. 6). Fig. 6(a) shows the stress–strain curves of the two kinds of

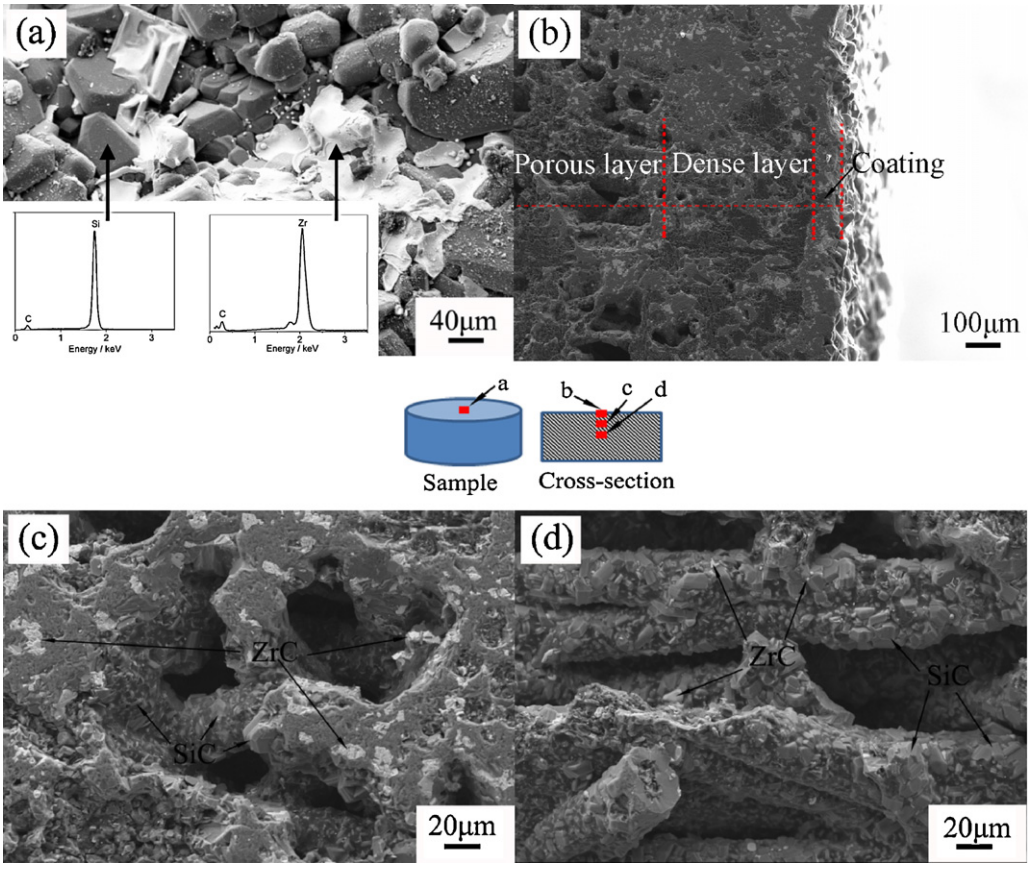

Fig. 4. SEM morphology and EDS analysis of integer felt reinforced C/C–SiC–ZrC composites: (a) surface; (b) cross-section; (c) inner fibers; (d) center fibers.

composites. It indicates that all composites present pseudo-plastic type damage without catastrophic failure in bending process. However, the fracture strain of C/C–SiC–ZrC composites decreases after infiltration. The morphology analysis of fracture surfaces of the composites are shown in Fig. 6(b). It is clear that pullout length of fibers of C/C–SiC–ZrC composites is much smaller than that of C/C composites, which validate the decrease of fracture strain in another way. Hence, the RMI process could affect the reinforcing effect.

3.3. Ablation properties of the composites

The dimension change of the samples before and after ablation test was measured to obtain the linear ablation rate. The mass ablation rate was determined by the weight change of the samples before and after ablation. The results are listed in Table 1. It can be seen that the mass and linear ablation rates of C/C–SiC–ZrC composites are much lower than those of C/C composites after ablation for 30 s. And within the 60 s of the

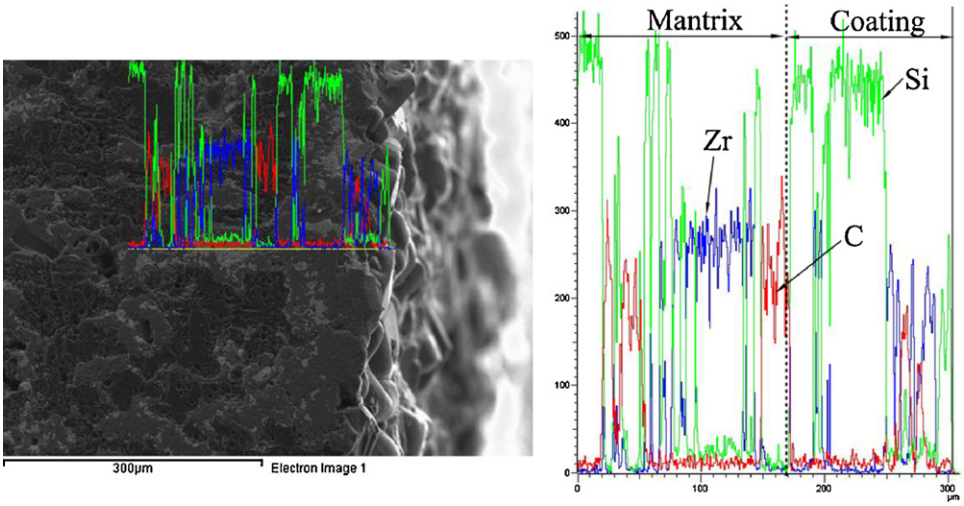

Fig. 5. Cross-section linear EDS analysis of the integer felt reinforced C/C–SiC–ZrC composites.

Table 1
Density, mechanical and ablation properties of the C/C composites and C/C–SiC–ZrC composites.

Materials	Initial density (g/cm^3)	Final density (g/cm^3)	Bending strength (MPa)	Linear ablation rate ($\times10^{-3}$ mm/s)			Mass ablation rate ($\times10^{-3}$ g/s)		
				20 s	30 s	60 s	20 s	30 s	60 s
C/C	1.35	1.35	50.39	–	3.00	–	–	1.13	–
C/C–SiC–ZrC	1.35	2.04	55.09	0.50	2.33	2.67	−0.01	0.69	0.57

test, the linear ablation rate of the C/C–SiC–ZrC composites increased with time and the mass ablation rate increased firstly and then decreased.

3.4. Ablation process and mechanism of the composites

Fig. 7 shows the morphology and EDS analysis of two kinds of composites in the center and outer region after ablation for different times. The erosion morphology of ablation center region of C/C composites after ablation for 30 s is shown in Fig. 7(a) and (b). Through the comparison with Fig. 2(a) and (b), it is found that grievous erosion occurred at the weak points, such as voids, cracks, carbon fibers and fiber–matrix interfaces. The carbon fibers became rough and the voids enlarged because of the oxidation and denudation during the ablation process. However, the ablation surface of the integer felt reinforced C/C composites is very smooth without typical ablation crater.

The morphology and EDS analysis of the C/C–SiC–ZrC composites after ablation for different times are shown in Fig. 7(c)–(h). At the ablation center (Fig. 7(c), (e) and (g)), there is a glass-like protective layer. XRD and EDS patterns of the ablated samples (Figs. 3, 7(e) and (g)) indicate that the glass-like layer consists of a mixture of ZrO_2 and SiO_2. Hence, it can be deduced that the following reactions would happen during the ablation process [9,18–20]:

$$SiC(l) + 2O_2(g) = SiO_2(l) + CO_2(g) \quad (3)$$

$$2SiC(l) + 3O_2(g) = 2SiO_2(l) + 2CO(g) \quad (4)$$

$$2SiO_2(l) + SiC(l) = 3SiO(g) + CO(g) \quad (5)$$

$$ZrC(s) + 2O_2(g) = ZrO_2(s) + CO_2(g) \quad (6)$$

$$2ZrC(s) + 3O_2(g) = 2ZrO_2(s) + 2CO(g) \quad (7)$$

According to the above formulas, ZrC and SiC will react with oxygen in the flowing gas to form ZrO_2 and SiO_2 during the ablation process. It is well known that ZrO_2 usually exhibits a loose and porous structure. However, ZrO_2 could be more stable on the ablated surface with the aid of SiO_2 melt [21]. In addition, the center of the ablated sample has the highest temperature of about 2300 °C, where SiO_2 and ZrO_2 can be sintered together to form a dense layer that can block the conducted heat and resist the ultrahigh temperature scouring of oxyacetylene flame. At the beginning of the ablation, the

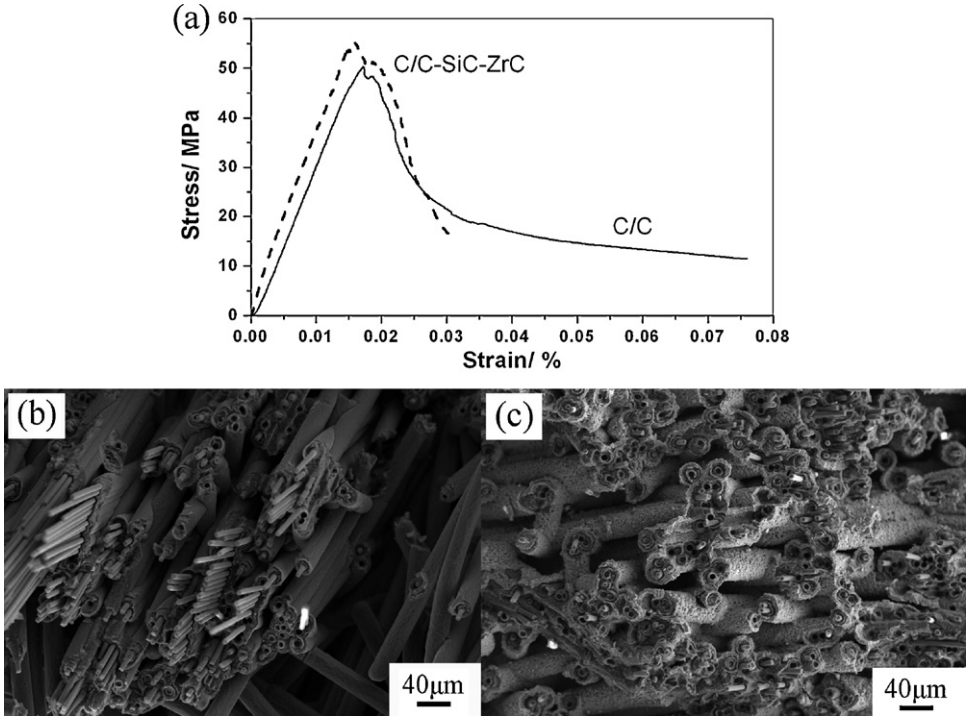

Fig. 6. Mechanical properties of C/C and C/C–SiC–ZrC composites: (a) stress–strain curves of bending load; (b) SEM photograph of fracture surface of C/C composites; (c) SEM photograph of fracture surface of C/C–SiC–ZrC composites.

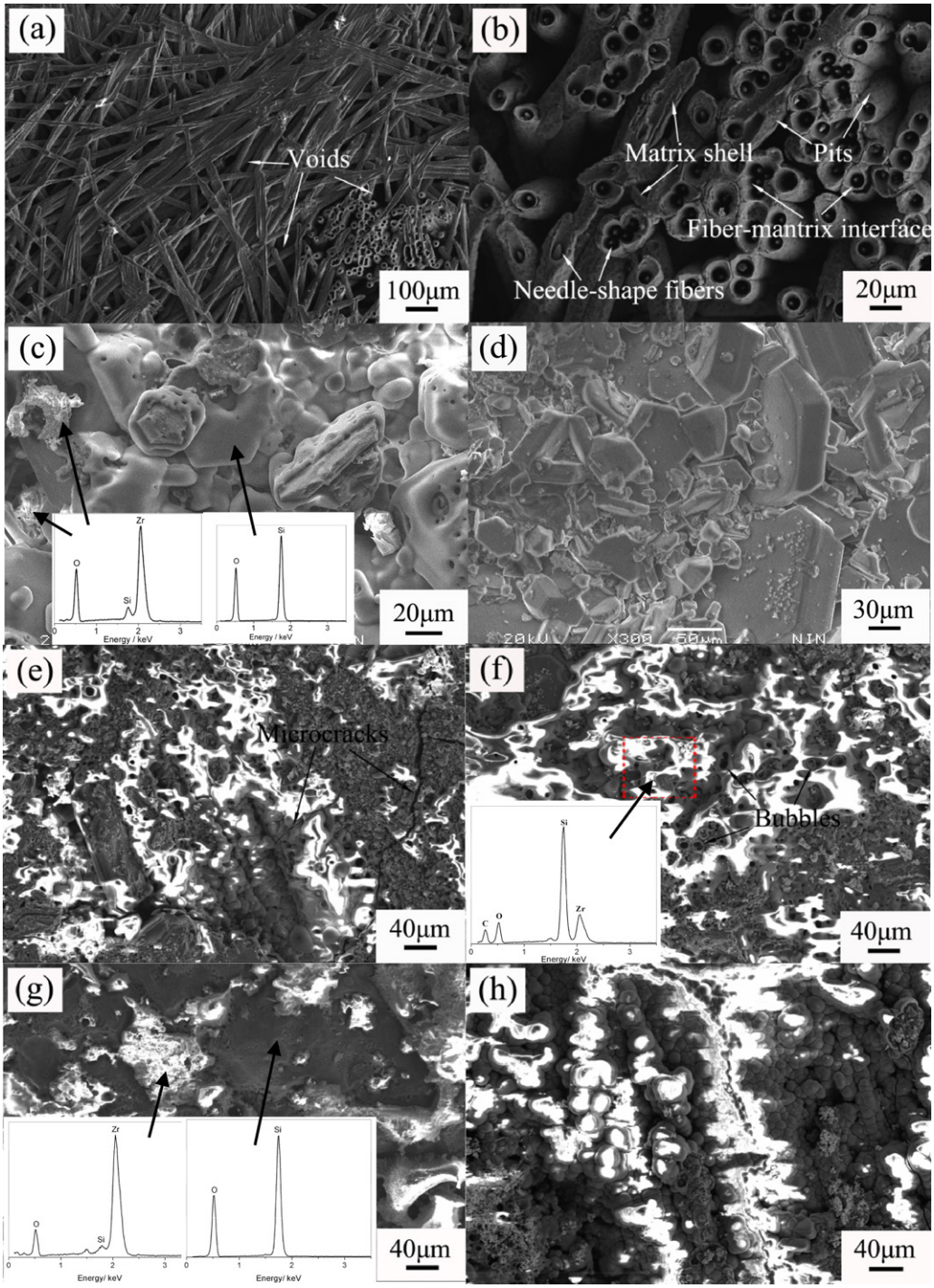

Fig. 7. Ablation morphology and EDS analysis of two kinds of composites after ablation for different time: center region of C/C composites after ablation for 30 s (a) and (b); center and outer region of C/C–SiC–ZrC composites after ablation for 20 s (c) and (d), for 30 s (e) and (f), and for 60 s (g) and (h).

oxidation of SiC and ZrC led to a net mass gain due to the dominance of the passive thermal–chemical reaction on the surface of the samples, so the mass ablation rate is negative and the surface of the sample is slightly ablated in the first 20 s (Table 1 and Fig. 7(c)). With the ablation time extending, the dense oxide layer was later destroyed because of the extravasation of CO and SiO (Reaction (5)) and the denudation by high temperature and high speed flame. Then the SiC layer beneath the as-destroyed SiO_2 film was exposed, and a new SiO_2 film would be formed on the SiC coating surface as a result of Reactions (3) and (4). Through the process of these cycles, the alternate occurrence of the gasification and regeneration of SiO_2 film resulted in the decreasing thickness and mass of the composites (Table 1). Moreover, the evaporation of the SiO_2 melt occurred and consumed most of the conducted heat in this area. As is indicated by Fig. 7(g), there is a larger content of ZrO_2 remaining after ablation for 60 s due to the oxidation and denudation of SiC on the surface of coating, which is helpful to

resist the further ultrahigh temperature scouring of oxyacetylene flame to the molten SiO_2 layer. Some microcracks can be seen in the ablation center region (Fig. 7(e)), but they might be self-sealed when the sample was heated again due to their small size and the good fluidity of SiO_2 glass at high temperature. Therefore, they have little effect on the ablation protection of the composites.

In the outer region near to the ablated center (Fig. 7(d), (f) and (h)), the surface of the composites is covered by a white layer which has a very different morphology due to a different ablation time. The samples in this area endure lower temperature, flow rate and pressure compared with the center region due to the deviation from oxyacetylene flame center. Thus, the effect of ablation behaviors is weakened. It can be seen that the layer is very thin after ablation for 20 s and the surface of the composites is slightly oxidized, which may be caused by that the ablation time was short and the temperature of composite surface had not reached the value needed for active oxidizing reaction. After ablation for 30 s, there are glass phases with some bubbles and pores in this area (Fig. 7(f)). The EDS analysis indicates that the glass phases are SiO_2 combined with ZrO_2. The layer of the mixture of SiO_2 and ZrO_2 can prevent the samples from being further ablated. It could be deduced that oxidation of SiC becomes active according to Reactions (3) and (4) and the volatilization of SiO according to Reaction (5) results in the bubbles on the surface. As is shown in Fig. 7(h), a dense oxide layer can be seen on the surface after ablation for 60 s. It can be inferred that with the extension of ablation time, the SiO_2 and ZrC generated by the reactions increased gradually in amount and was not scoured off by flux due to the low speed and low pressure of the flame here. This dense oxide layer could effectively protect the samples from further ablation under oxyacetylene flame.

4. Conclusions

A kind of integer felt reinforced C/C–SiC–ZrC composites was prepared by isothermal chemical vapor infiltration (ICVI) combined with reaction melt infiltration (RMI) method in this study. The composites obtained consisted of C, SiC, and ZrC. There is a dense ZrC–SiC coating formed on the surface of the composites as well as on the surface of the individual fibers. The ablation properties of the composites were tested by an oxyacetylene flame for 20 s, 30 s and 60 s. The morphology of the ablated samples was analyzed. The results indicate that integer felt reinforced C/C–SiC–ZrC composites possess better ablation properties than C/C composite ablated for 30 s, and the linear and mass ablation rates of the C/C–SiC–ZrC composites after ablation for 60 s are 2.67×10^{-3} mm/s and 0.57×10^{-3} g/s, respectively. The dense ZrC–SiC coating and its glass-like oxide layer formed during ablation process effectively enhance the ablation resistance of the composites.

Acknowledgements

This work has been supported by the National Natural Science Foundation of China under Grant Nos. 50902111 and 50972120, the Research Fund of State Key Laboratory of Solidification Processing (NWPU), China (Grant Nos. G8QT0222 and 25-TZ-2009).

References

[1] E. Fitzer, The future of carbon/carbon composite, Carbon 25 (1987) 163–190.
[2] H.J. Li, Carboncarbon composites, New Carbon Mater. 16 (2001) 79–80.
[3] J.D. Buckley, Carbon–carbon materials and composite, NASA Reference Publication, NASA Lewis Research Center, 1992, pp. 267–281.
[4] D.L. Schmidt, K.E. Davidson, L.S. Theibert, Unique application of carbon–carbon composites, SAMPE J. 35 (1999) 27–39.
[5] Y. Yang, J. Yang, D. Fang, Research progress on thermal protection materials and structures of hypersonic vehicles, Appl. Math. Mech. 29 (2008) 51–60.
[6] R. Savino, Aerothermodynamic study of UHTC-based thermal protection systems, Aerosp. Sci. Technol. 9 (2005) 151–160.
[7] J.E. Sheehan, Oxidation protection for carbon fiber composites, Carbon 27 (1989) 709–715.
[8] W.G. Fahrenholtz, G.E. Hilmas, Future ultrahigh temperature materials. UHTM Workshop Draft Report NSF-AFOSR Joint Workshop on Future Ultra-High Temperature Materials, 2004.
[9] X.T. Shen, K.Z. Li, H.J. Li, H.Y. Du, W.F. Cao, F.T. Lan, Microstructure and ablation properties of zirconium carbide doped carbon/carbon composites, Carbon 48 (2010) 344–351.
[10] X.T. Li, J.L. Shi, G.B. Zhang, H. Zhang, Q.G. Guo, L. Liu, Effect of ZrB_2 on the ablation properties of carbon composites, Mater. Lett. 60 (2006) 892–896.
[11] Q.F. Tong, J.L. Shi, Y.Z. Song, Q.G. Guo, L. Liu, Resistance to ablation of pitch-derived ZrC/C composites, Carbon 42 (2004) 2495–2500.
[12] D.D. Jayaseelan, R.G. Sá, P. Brown, W.E. Lee, Reactive infiltration processing (RIP) of ultra high temperature ceramics (UHTC) into porous C/C composite tubes, J. Eur. Ceram. Soc. 31 (2011) 361–368.
[13] W. Qiang, Zirconium, Mechanical Industry Publishing Company, China, 1961
[14] E.K. Storms, The Refractory Carbides, Academic Press, New York, 1967.
[15] Y.G. Wang, X.J. Zhu, L.T. Zhang, L.F. Cheng, Reaction kinetics and ablation properties of C/C–ZrC composites fabricated by reactive melt infiltration, Ceram. Int. 37 (2011) 1277–1283.
[16] Y.L Zhang, H.J. Li, X.Y. Yao, K.Z. Li, X.F. Qiang, Oxidation protection of C/SiC coated carbon/carbon composites with Si–Mo coating at high temperature, Corros. Sci. 53 (2011) 2075–2079.
[17] L.H. Zou, N. Wali, J.M. Yang, N.P. Bansal, Microstructural development of a Cf/ZrC composite manufactured by reactive melt infiltration, J. Eur. Ceram. Soc. 30 (2010) 1527–1535.
[18] Y.J. Song, G.M. Wang, Y. Zhou, Elevated temperature ablation resistance and thermophysical properties of tungsten matrix composites reinforced with ZrC particles, J. Mater. Sci. 36 (2001) 4625–4631.
[19] W. Sun, X. Xiong, B.Y. Huang, G.D. Li, H.B. Zhang, Z.K. Chen, X.L. Zheng, ZrC ablation protective coating for carbon/carbon composites, Carbon 47 (2009) 3368–3371.
[20] J.S. Wang, Z.P. Li, M. AO., Z.H. Xu, L. Liu, Z.J. Hu, W.Z. Peng, Effect of doped refractory metal carbides on the ablation mechanism of carbon/carbon composites, New Carbon Mater. 21 (2006) 9–13.
[21] Q.M. Liu, L.T. Zhang, J. Liu, X.G. Luan, L.F. Cheng, Y.G. Wang, The oxidation behavior of SiC–ZrC–SiC coated C/SiC minicomposites at ultrahigh temperatures, J. Am. Ceram. Soc. 93 (2010) 3990–3992.